RSC Advances

PAPER

View Article Online
View Journal | View Issue

Cite this: *RSC Adv.*, 2016, **6**, 87910

Aptamer mediated niosomal drug delivery†

Didem Ag Seleci, Muharrem Seleci, André Jochums, Johanna-Gabriela Walter, Frank Stahl* and Thomas Scheper

Received 2nd August 2016
Accepted 4th September 2016

DOI: 10.1039/c6ra19525c

www.rsc.org/advances

Development of nanoscale carrier systems for targeted drug delivery is crucial for cancer treatment. The current methods of drug delivery exhibit some problems such as lack of therapy efficiency at the desired parts of the body, degradation of the drug before reaching the desired tissue and limitations in cellular penetration. In this work, a novel drug delivery platform was developed to overcome these problems and to enable specific and efficient uptake into the cells. The surface of the synthesized polyethylene glycolated niosomes (PEGNIO) was modified with cell penetrating peptide (CPP) and cell specific MUC1 (S2.2) aptamer, and doxorubicin (DOX) as a cancer model drug was encapsulated in this platform. Fluorescence microscopy and flow cytometry analysis were used to investigate the cellular uptake and intracellular distribution of the DOX loaded niosomal formulation. *In vitro* cytotoxicity studies were carried out using MUC1 positive HeLa and negative U87 cells. Moreover, dynamic light scattering (DLS), zeta potential measurements and fluorescence absorption spectroscopy were performed to determine the vesicle size, as well as charge and spectroscopic properties of the conjugates. From these results, this novel aptamer mediated niosomal drug delivery platform may have application potential in targeted drug delivery towards MUC1-overexpressing tumors.

Introduction

A drug delivery system (DDS) is described as a formulation that enables the introduction of drug molecules into the body with improved efficacy and safety. Due to the rapid progress of nanotechnology, numerous nanocarriers have been developed to securely deliver drugs into target sites. New targeting agents, including aptamers, short peptides, and small molecules have recently become promising targeting ligands to design novel drug delivery systems.

The current treatment options for cancer are surgical operation, radiation and chemotherapy or a combination. The therapeutic efficacy of many anticancer drugs is limited by their poor penetration into tumor tissue and by their side effects on healthy cells.[1] To overcome these limitations, development of a novel carrier platform for specific drug uptake into the cell with an optimal dose at high efficiency is important. Therefore, anticancer drugs can be conjugated with biomolecules exhibiting potential for cellular targeting and penetration and can be delivered to the desired site of action by multi-functional carrier platforms. Vesicular nanocarriers have received great attention as potential drug carrier systems. Nonionic surfactant based vesicles "niosomes" are one class of vesicular nanocarriers which can accommodate a large number of drugs with a wide range of solubility.[2–4] Due to their low cost, long term storage stabilities and lower toxicity of niosomes have been used for drug delivery.[5–7] The addition of polyethylene glycol (PEG) to the nanocarrier surface increases the steric stabilization of the nanoparticle and allows for further surface modifications to design specific drug delivery systems. It is generally thought that PEGylation protects the delivery systems against the immune system and thereby prolong circulation life times.[8]

In solid tumors, the penetration of the tissue by the anticancer drug is limited which causes reduced efficacy and the development of drug resistance.[9] A promising approach to overcome the cellular barrier is based on the use of certain peptides namely cell penetrating peptides (CPPs), able to translocate across the cell membrane and deliver their payload intracellularly within minutes.[10] CPPs consist of small cationic or amphipathic peptides that aid the uptake of attached cargos into living cells. A wide variety of small molecules and biomolecules including plasmid DNA, siRNA, oligonucleotides and peptide nucleic acid molecules have been attached to these peptides and were subsequently internalized.[11–13] The ability of CPPs to translocate biologically active molecules into cells makes these peptides promising candidates for theranostic applications.[14] TAT is one of the smallest polycationic CPPs composed of arginine and lysine residues. Studies on the binding affinities of cationic TAT peptides indicate that these peptides strongly bind electrostatically to the various anionic species (*e.g.* heparan sulphate proteoglycans) present at the extracellular surface of cell membranes.[15,16] The exact molecular mechanism of cellular entry of CPPs is currently not fully

Institute of Technical Chemistry, Leibniz University Hannover, Callinstreet 5, 30167 Hannover, Germany. E-mail: stahl@iftc.uni-hannover.de

† Electronic supplementary information (ESI) available. See DOI: 10.1039/c6ra19525c

understood. Former studies indicated that in general uptake occurs by endocytosis (or more specifically macropinocytosis) and direct membrane translocation.[17] The lack of cell specificity remains the major drawback for the clinical application of CPPs.[18]

Receptors that are over-expressed in many cancer cells are suitable targets to achieve a more specific delivery. MUC1 is a large transmembrane glycoprotein overexpressed in most malignant adenocarcinoma, including ovarian, lung, pancreatic, prostate, and breast cancers, making it an ideal target molecule for chemotherapeutics.[19] Aptamers are short oligonucleotides that are capable to selectively bind their corresponding target.[20–22] These reagents are selected by an *in vitro* process called SELEX, (systematic evolution of ligands by exponential enrichment).[23] Several MUC1 aptamers were developed by Ferreira *et al.* and S2.2 is a 25-nucleotide truncated version of the original MUC1 aptamer. It binds MUC1 protein with high specificity and affinity with a K_D of 0.135 nM.[24,25] S2.2 has been used in a few targeted delivery systems. Yu *et al.* used MUC1 aptamer to target paclitaxel (PTX) loaded poly(lactic-*co*-glycolic-acid) (PLGA) nanoparticles.[26] Furthermore PEG-modified MUC1 targeting doxorubicin (DOX) was designed and the aptamer–doxorubicin complex was prepared by intercalation of the aptamer with DOX by Tan *et al.*[27] Recently, Liu *et al.* synthesized vinorelbine (VRL) loaded and MUC1 aptamer modified lipid–polymer hybrid nanoparticles.[22]

In this study, polyethylene glycolated niosomes (PEGNIO) were prepared from span60, cholesterol and 1,2-distearoyl-*sn*-*glycero*-3-phosphoethanolamine-*N*-[maleimide (polyethylene glycol)-2000] (DSPE-PEG(2000) Maleimide). DOX was encapsulated into the PEGNIO. The niosomes were characterized with respect to size, morphology and drug encapsulation efficiency. Cysteine-modified cell penetrating peptide (CysTAT) was conjugated to the amine group of MUC1 aptamer in the presence of a crosslinking agent bis(sulfosuccinimidyl)suberate (BS3). Subsequently CysTAT–MUC1 conjugate was attached to DOX encapsulated PEGNIO (PEGNIO/DOX) *via* the formation of a thioether linkage. The anticancer activity of DOX-loaded targeted vesicles was studied in HeLa (cervical cancer cells) and U87 (human glioblastoma cells) cell lines by evaluating the cellular uptake and cytotoxicity. The designed nanoparticular drug delivery system composed of aptamer–CPP–PEGNIO was first fabricated in this study. Our findings suggest that this platform can serve as a delivery vehicle for cancer cells over-expressing MUC1.

Materials and methods

Materials

Amine and Cy5 modified MUC1 aptamer S2.2 (5′-NH_2-GCA GTT GAT CCT TTG GAT ACC CTG G-3′), (5′-Cy5-GCA GTT GAT CCT TTG GAT ACC CTG G-3′) were purchased from Integrated DNA Technologies. CysTAT with CYGRKKRRQRRR–NH_2 sequence was obtained from GenScript. DSPE-PEG(2000) Maleimide was provided by Avanti. Span60, cholesterol, 3-(4,5-dimethylthiazol-2-yl)-2,5-diphenyl tetrazoliumbromide (MTT), 4,6-diamino-2-phenylindol (DAPI) and Dulbecco's Modified Eagle Medium (DMEM) were ordered from Sigma Aldrich. RNAtidy G and sodium dodecyl sulfate (SDS) were purchased from Applichem. BS3 was ordered from Covachem. Doxorobucin (hydrochloride) was purchased from Cayman Chemical. GeneRuler 100 bp DNA ladder and dNTP Set (100 mM solutions) were obtained from Fermentas. M-MLV reverse transcriptase and its M-MLV RT 5× buffer as well as GoTaq polymerase and its 5× Green GoTaq reaction buffer were provided from Promega. PCR primers were synthesized by Life Technologies.

Preparation of PEGylated niosomes

Multi lamellar vesicles (MLVs) of PEGNIO were prepared by the thin film hydration method.[28] Span 60, cholesterol, and DSPE-PEG(2000) Maleimide were dissolved in 1.0 mL chloroform in a round-bottom flask with the molar ratio of 4.95 mM : 4.95 mM : 0.1 mM. The solvent was evaporated with constant rotation at 38 °C under reduced pressure to form a thin lipid film. Then the thin film was hydrated with 1.0 mL of distilled water for preparing empty niosomes, or a doxorubicin solution (0.22×10^{-3} M in water) to obtain PEGNIO/DOX conjugate at 60 °C for 60 min. Afterward the niosomal suspension was equilibrated at room temperature overnight, to complete annealing and partitioning of the drug between the lipid bilayer and the aqueous phase.[5] Small unilamellar vesicles (SUVs) were prepared starting from MLVs by extruding the niosomes 11 times through 0.4 μm and 0.1 μm pore size polycarbonate filters using mini-extruder set (Avanti polar lipids). Niosomes were purified by dialysis against water for 3 h using 6–8 kDa dialysis bag.

Synthesis and characterization of CysTAT–MUC1 conjugate

The conjugation between CysTAT and amine modified MUC1 aptamer was performed using an amine to amine crosslinker BS3. 35 μL containing 5 nmol amine modified MUC1 aptamer, 30 μL containing 20 nmol CysTAT peptide and 150 μL containing 1.75 μmol BS3 were mixed in 85 μL 0.1 M sodium phosphate including 0.15 M sodium chloride at pH 7.4 and incubated at room temperature for 1 h. Once the reaction was completed, 300 μL 1.0 M Tris buffer was added to quench the reaction for 20 minutes at room temperature. Unreacted peptides and quenched crosslinkers were removed through dialysis against PBS (pH 7.2) using 3.5 kDa dialysis bag. During this reaction aptamer–aptamer and peptide–peptide conjugation can occur. Denaturing urea polyacrylamide gel electrophoresis (Urea PAGE) and HPLC were used for the characterization of CysTAT–MUC1. Urea PAGE was performed according to manufacturer's instructions (QIAGEN). Briefly 15% acrylamide/urea gel was prepared and run for 30 min at 200 V. The samples were heated at 95 °C for 2 min and then they were immediately transferred onto ice. The samples were loaded onto the gel and the gel was run for 1.5 h at 200 V. Afterward the gel was stained with methylene blue solution and documented using an INTAS UV documentation system. HPLC measurements and carried out using VWR Hitachi Chromaster. For the analysis, a DAD detector and Kinetix 2.6 μm C8 100 Å, 150 × 4.6 mm (Phenomenex) column were used. Detection was performed at 214 nm at room temperature. The mobile phase

consisted of 0.065% trifluoroacetic acid (TFA) in water and 0.05% TFA in acetonitrile with a flow rate of 1.0 mL min^{-1}.

Conjugation CysTAT–MUC1 to PEGNIO/DOX

CysTAT–MUC1 was conjugated to PEGNIO/DOX *via* thiol group of cysteine to maleimide group on PEGNIO resulting in the formation of a thioether linkage.[29,30] Maleimide group reacts specifically with thiol-groups in the pH range 6.5–7.5. 100% of the prepared CysTAT–MUC1 conjugate in PBS (pH 7.2) and 50% of the prepared PEGNIO/DOX were mixed and incubated overnight at room temperature. After completing the reaction between sulfhydryl group of CysTAT and maleimide group of DSPE-PEG(2000) Maleimide, the final PEGNIO/DOX/CysTAT–MUC1 conjugate was purified using 14 kDa dialysis bag to remove unbound CysTAT–MUC1. Schematic representation of niosome synthesis, drug encapsulation and the bioconjugation processes are shown in Scheme 1.

Measurement of particle size, distribution and zeta potential

Size, size distribution and zeta potential of niosomes were determined by dynamic light scattering (DLS) analysis using Malvern Zetasizer Nanoseries-Nano-ZS. The polydispersity index (PDI) was used as a measure of the width of size distribution. PDI less than 0.3 corresponds to a homogenous population for colloidal systems.[31] Each sample was measured three times.

Stability

The stability of DOX loaded niosomal formulations was tested *via* DLS analysis. After the synthesis of PEGNIO/DOX and PEGNIO/DOX/CysTAT–MUC1, these conjugates were stored at 4 °C in the dark. The particle size and PDI values were measured for 2 months. Additionally the particle size of PEGNIO/DOX/CysTAT–MUC1 was measured in cell culture media before and after the incubation at 37 °C for 24 h.

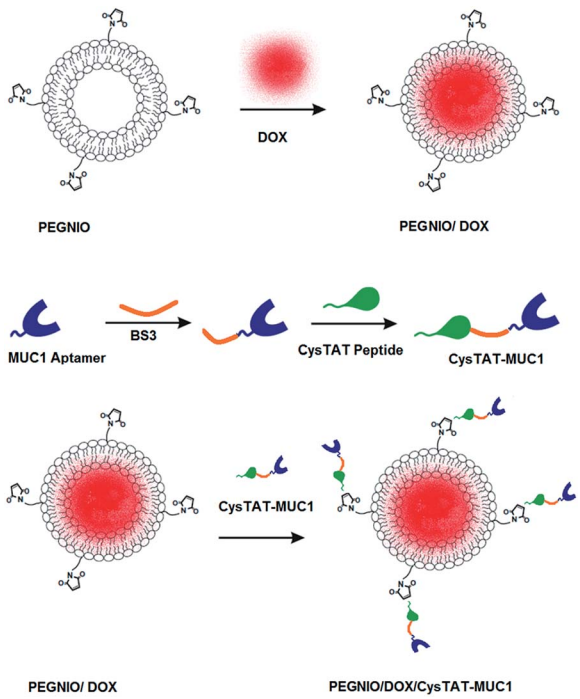

Scheme 1 Schematic representation of drug the encapsulation and the bioconjugation process.

Entrapment efficiency

The drug encapsulation efficiency was determined using the dialysis technique.[32] According to this method, directly after the preparation 1.0 mL of PEGNIO/DOX and 1.0 mL of PEGNIO/DOX/CysTAT–MUC1 dispersions were dropped into two dialysis bags (12–14 kDa) and immersed in 100 mL of distilled water with magnetic stirring at 100 rpm. Samples were dialyzed for 3 h. The percent of encapsulation efficiency (E%) was expressed as the percentage of the drug entrapped in niosomes (and thus not removed *via* dialysis) referred to the initial amount of drug that is present in the nondialyzed sample. It was determined by diluting 50 μL of dialyzed and 50 μL of nondialyzed niosomes in 1.0 mL of methanol. This step is essential for breaking the niosomal membrane, thereby releasing the entrapped DOX. Subsequently, the amount of DOX was determined by HPLC using a C18 column (Phenomenex Kinetix, 4.6 × 100 mm, 2.6 μm) at 35 °C and a UV detector was conducted at 254 nm. The mobile phase consisted of methanol and water (60/40, v/v) containing 0.1% formic acid and 0.1% ammonia solution (25%) with a flow rate of 1.0 mL min^{-1}.[33] The stock solutions of DOX were prepared at 1.0 mg mL^{-1} in methanol and further diluted with methanol in the concentration range 1.0–200 μg mL^{-1}. The amount of encapsulated DOX was calculated according to the calibration curve ($y = 120\,777x - 67\,040$, $R^2 = 0.9984$). The limit of detection (LOD) and limit of quantification (LOQ) for DOX were found to be 6.12 μg mL^{-1}, 18.55 μg mL^{-1} respectively based on 3.3σ/slope and 10σ/slope formulations.[34]

Drug release

Drug release experiments were performed using the dialysis method. The DOX-loaded niosome solutions were prepared and transferred into a dialysis membrane tubing (Thermo, Slide-ALyzer MINI Dialysis Devices, 10k MWCO). The tubing was immersed in 10 mL of the PBS buffer (pH 5.6 and 7.4), placed in an incubator at 37 °C and stirred at 100 rpm. At specific time intervals, 0.5 mL samples were removed from the release medium and replaced with the same volume of fresh buffer. A calibration curve was established with a known concentration of free DOX by fluorescence emission measurements at 595 nm using NanoDrop 3300. The amount of released DOX was calculated according to the calibration curve ($y = 254.93x - 30.74$, $R^2 = 0.9960$, LOD = 0.61 μg mL^{-1}, LOQ = 1.84 μg mL^{-1}).

Cell culture

HeLa and U87 cell lines were provided from German Collection of Microorganisms and Cell Cultures (DSMZ). Both cell lines were grown in DMEM containing 10% fetal calf serum (FCS) and 1.0% penicillin/streptomycin (P/S). All cells were cultivated in medium and incubated with samples and reagents at 37 °C in a humidified environment with 5.0% CO_2.

MUC1 expression on cell surfaces

PCR and flow cytometry analysis were used to confirm expression of the MUC1 receptor in HeLa and lack of expression in U87 cells. Total cellular RNA of the cells was isolated using Trizol reagent (Invitrogen) and transcribed into cDNA. The primers were designed with Lasergene Primer Select Software using the NCBI reference mRNA sequence for *Homosapiens* mucin 1, cell surface associated (MUC1), transcript variant 1 (NM_002456.5). The primer sequences are as follows: MUC1 forward 5′-TAC CGA TCG TAG CCC CTA TG-3′ and reverse 5′-CCA CAT GAG CTT CCA CAC AC-3′. The human housekeeping gene hypoxanthine phosphoribosyltransferase (HPRT) was additionally used to prove the successful synthesis of cDNA. The primer sequences are: HPRT forward 5′-AAG CTT GCT GGT GAA AAG GA-3′ and reverse 5′-AAG CAG ATG GCC ACA GAA CT-3′. The protocol described in our previous publication was used in the polymerase chain reactions.[35] The annealing temperature of 60 °C was used for MUC1 and HPRT during PCR experiments. PCR products were separated in 1.5% agarose gel in TAE buffer and stained with 5.0 μL/100 mL buffer Roti-Safe Gel Stain ready to use by Thermo. The gel was run using the Thermo EC electrophoresis unit at 100 V for 60 min and documented using an INTAS UV documentation system.

For flow cytometry studies, 5×10^5 cells were collected. 100 μL of 5.0 μM Cy5 labelled MUC1 aptamer in PBS were added to the cells and the cell suspension was shaken at room temperature for 1 h with 500 rpm in the dark. The cells were washed once in 300 μL of PBS to remove unbound aptamer. Before flow cytometric analysis, cells were resuspended in 500 μL of PBS and the stained cells were analyzed in a BD Accuri C6 flow cytometer. At least 20 000 gated events were observed in total and living cells were gated in a dot plot of forward *versus* side scatter signals. For drawing dot plots and histograms the BD Accuri C6 software was used.

Cytotoxicity

3-(4,5-Dimethylthiazol-2-yl)-2,5-diphenyl tetrazolium bromide (MTT) assays were used to determine cytotoxicity of the niosomal formulations. Cells (8×10^3) were seeded out in 96-well tissue plates (Sarstedt, USA) in a volume of 200 μL and cultivated for three days. After this cultivation time cells were washed once in PBS and treated with SUVs (PEGNIO, PEGNIO/DOX, PEGNIO/DOX/CysTAT–MUC1) and free DOX for 24 h and 48 h. The equivalent concentration of free DOX was used in niosomal formulations. Then the samples were removed and cells were incubated in 110 μL per well 10% MTT solution (5.0 mg mL^{-1} in PBS) in medium for 4 h. During this incubation time, formazan complex was produced by the cells. 100 μL SDS solution (1.0 g SDS in 10 mL 0.01 M HCl) was added to each well to release the purple colored salt from the cells. After 24 h of incubation, UV-vis absorption was measured at 570 nm to 630 nm as the reference wavelength using a microplate reader Epoch Biotek.

Cellular uptake and internalization

The DOX uptake by HeLa and U87 cells for different DOX formulations was analyzed by flow cytometry. HeLa and U87 cells were treated with PEGNIO/DOX, PEGNIO/DOX/CysTAT–MUC1 and free DOX for 2 h and treated cells were washed two times with PBS, and then analyzed in a BD Accuri C6 flow cytometer.

Cellular internalization of PEGNIO/DOX/CysTAT–MUC1 was determined *via* fluorescence microscopy studies. HeLa and U87 cells were cultivated for 2 days on the chamber slides (μ slides 8 well purchased at ibidi GmbH) in a volume of 200 μL of the medium. PEGNIO/DOX/CysTAT–MUC1 was diluted with medium and then added to the cells. The cells were incubated for 4 h at 37 °C and washed once in PBS. Afterward 100 μL DAPI solution (1.0 μg mL^{-1}) was added to the cells and incubated for 15 min. After DAPI staining, the cells were washed with PBS once. Images were taken using an OLYMPUS BX41 fluorescence microscope equipped with an OLYMPUS SC30 camera.

Statistical analysis

Statistical analysis was performed using the GraphPad InStat statistical software. All experiments were repeated three times. The paired *t*-test was performed. The difference between two groups was considered to be significant when the p value was less than 0.05.

Results

Doxorubicin is one of the most extensively used broad-spectrum anticancer drugs. It accumulates inside the cell nucleus where it intercalates into DNA and inhibits the progression of topoisomerase II to cause DNA damage and cleavage.[36,37] Long treatment durations and toxic side effects are inconvenient in the use of conventional chemotherapeutics.[38] Recent studies show that, biocompatible nanoparticles, with an increased surface area to volume ratio can overcome non-cellular and cellular-based mechanisms of resistance and increase the selectivity of drugs towards cancer cells, while reducing their toxicity towards normal tissues.[39] The addition of PEG to the nanoparticle surface prolongs vesicles residence time in blood and accumulation at the pathological sites.[5] Taking this into consideration, we decided to use PEGylated niosomes for obtaining aptamer targeted-cell penetrating vesicular systems.

Conjugation and characterization of CysTAT–MUC1

BS3 is an amine reactive, homobifunctional, sulfo-NHS ester, crosslinking reagent.[40] The reactivity of the sulfo-NHS esters is highly reactive toward amines in the pH range of 7–9. The amine modified MUC1 aptamer was reacted with the $-NH_2$ group in the CysTAT peptide in the presence of BS3 to produce the CysTAT–MUC1 conjugates. Besides the desired conjugate CysTAT–MUC1, the reaction can also result in dimers of MUC1 aptamer and peptide. In order to investigate the product spectrum of the crosslinking reaction, gel electrophoresis was performed. Free MUC1 aptamer and CysTAT–MUC1 were applied to Urea PAGE. A single band was observed for free aptamer. In the case of CysTAT–MUC1 conjugate double bands were observed (Fig. S1†). In the double bands, first band indicates CysTAT–MUC1 conjugate and the second one exhibits unbound

Table 1 Characterization of PEGNIO formulations incorporating DOX

Samples	Size (nm) intensity (%) (mean ± SD)	Polydispersity index (PDI)	Zeta potential (mV)	Entrapment efficiency (*E*%)
PEGNIO	151.0 ± 36	0.244	−4.96 ± 0.43	—
PEGNIO/DOX	152.7 ± 34	0.214	−3.56 ± 0.27	39.52 ± 1.8
PEGNIO/DOX/CysTAT–MUC1	164.5 ± 40	0.275	−8.62 ± 0.50	37.48 ± 2.1

aptamers in the conjugate. Additionally, the conjugation of aptamer and peptide was proven by HPLC analysis. For this aim, chromatograms of MUC1 aptamer, BS3 crosslinker, Cys-TAT peptide were compared with chromatogram of CysTAT–MUC1 conjugate (Fig. S2†). No peaks were observed for MUC1 aptamer in this HPLC method. CysTAT peptide and BS3 crosslinker have different retention times 7.75 and 8.67 respectively, showed that there is no interference during the analysis of the CysTAT–MUC1 conjugates. The conjugation efficiency was about 82% in accordance with the integrated areas of CysTAT peptide before and after conjugation. Besides CysTAT–MUC1, the conjugation can also result in aptamer and peptide dimers. Nonetheless, since these side products are not able to bind to maleimide group of PEGNIO (due to the lack of –SH group), we used to the as prepared conjugate with no additional purification.

Synthesis and characterizations of DOX loaded niosomal formulations

PEGylated niosomes were prepared by the thin film layer hydration technique, using span60:cholesterol:DSPE-PEG(2000) Maleimide. 0.22 mM doxorubicin solutions were used in the preparation of loaded vesicles. CysTAT–MUC1 was conjugated to PEGNIO/DOX to obtain targeted drug delivery system. The size of nanocarriers is very important for effective accumulation in tumor by enhanced permeability and retention effect (EPR) and cellular internalization. The mean diameters of empty and doxorubicin-loaded niosomal formulations, along with the corresponding polydispersity index (PDI), doxorubicin entrapment efficiency (*E*%) values, and zeta potential values are listed in Table 1. The empty vesicle size was analyzed to be 151.0 ± 36 nm. The hydrodynamic diameter did not change after DOX loading (152.7 ± 34 nm) but after conjugation with CysTAT–MUC1 it increased to 164.5 ± 40 nm. The stealth niosomes showed zeta potential values close to 0 mV but the surfaces of nanoparticles was grafted with PEG to improve water solubility and avoid aggregation.[5,41,42] Due to the presence of PEG in the niosome structure, no aggregation was observed. DOX loading influenced the zeta potential of the vesicles. The change in the zeta potential may be a result of DOX intercalation in the vesicle membrane.[5,43,44] Conjugation of CysTAT–MUC1 increased niosome size, corresponding with the presence of the aptamer on the niosomal surface increasing the hydrodynamic diameter. Moreover, the negatively charged DNA aptamer reduced the surface potential of the niosome.[29] PDI ranged from 0.275 to 0.214, demonstrating that the vesicle population is relatively homogeneous in size. The DOX entrapment efficacy (*E*%) was calculated to be around 39% and 37% for PEGNIO/DOX and PEGNIO/DOX/CysTAT–MUC1 respectively. The stability of niosomal DOX formulations was tested *via* DLS analysis and no changes were observed in the size and PDI values after two months storage at 4 °C in the dark (data not shown). Additionally, PEGNIO/DOX/CysTAT–MUC1 sample was diluted in cell culture media and was incubated at 37 °C for 24 hours. The size of the sample was measured before and after incubation and no changes were observed.

Drug release

Sustained drug release is one of the important properties of nanoscale drug delivery systems that will minimize side effects of the drug. In vesicular drug carrier systems, the drug release occurs by passive transport of the drug through the membrane bilayer.[45] The release of DOX from PEGNIO/DOX/CysTAT–MUC1 was investigated using dialysis methods at pH 7.4, which was chosen in accordance with physiological conditions and in an acidic environment (pH 5.6). The solutions were taken out at specific intervals and measured by fluorescence emission measurements at 595 nm to determine the amount of DOX that has been released. The *in vitro* DOX release profiles from PEGNIO/DOX/CysTAT–MUC1 showed the faster release of DOX under acidic environments than that at neutral pH (Fig. 1). Within 48 h, the release of DOX was 30% and 52% at pH 7.4 and pH 5.6 respectively. This can be explained by the higher solubility of DOX at the lower pH.[46] Especially, the pH change from 7.4 to 5.6 corresponds to the pH change from the normal

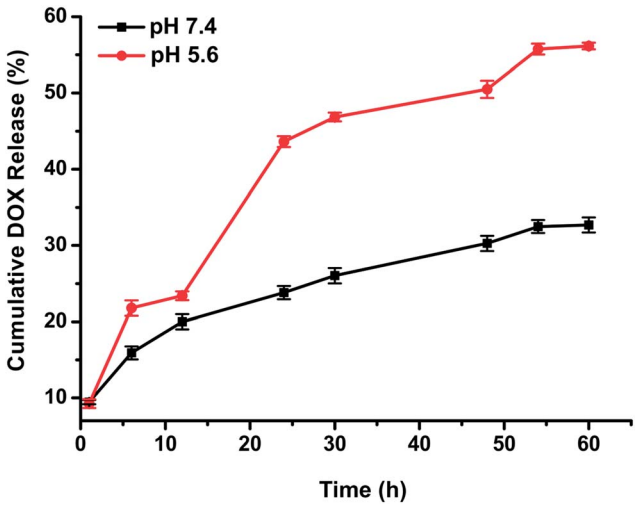

Fig. 1 *In vitro* cumulative release of DOX from PEGNIO/DOX/CysTAT–MUC1 at pH 7.4 and 5.6.

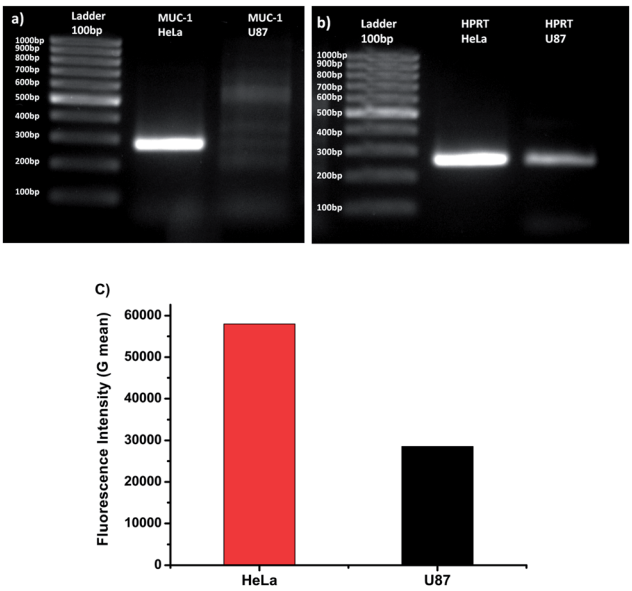

Fig. 2 Image of 1.5% agarose gel with results of PCR for HPRT gene and MUC1 expression in HeLa and U87 cells (a and b). Flow cytometry analysis of MUC1 expression on HeLa and U87 cells using Cy5-labelled aptamer S2.2 (c).

physiological environment in body circulation to the intracellular tumor tissue. According to results this conjugate is expected to be a promising drug delivery system for the tumor-targeted delivery of DOX.

Confirmation of MUC1 receptor expression on the cell surface

To test PEGNIO/DOX/CysTAT–MUC1 as a targeted drug delivery system *in vitro*, first the expression of MUC1 was evaluated in HeLa and U87 cells. Gene expression of MUC1 was investigated at the mRNA level using polymerase chain reaction (PCR) and at the cell surface protein level using flow cytometry. Agarose gel analysis with the results of PCR experiments is shown in Fig. 2. The housekeeping gen (HPRT) was measured as a control for both HeLa and U87 cells (Fig. 2a and b). Bands corresponding to housekeeping genes were observed for both cell types (263 bp) confirming the success of RNA extraction and PCR. Fig. 2a demonstrates that HeLa cells show a high level of transcription of the MUC1 gene, which results in a strong band at the expected base pair length of 283 bp. No corresponding band was observed in U87 cells, thereby indicating the lack of expression of MUC1. The PCR results were also confirmed by using Cy5 labeled MUC1 aptamer in flow cytometry. Cells were treated with a Cy5 labeled MUC1 aptamer. After the treatment, the mean fluorescence intensity was measured to be 28 523 for U87 cells, and 57 993 for HeLa cells (Fig. 2c). Both methods confirmed that MUC1 expression was considerably higher in HeLa cells than in U87 cells. These results are in agreement with the literature.[47,48]

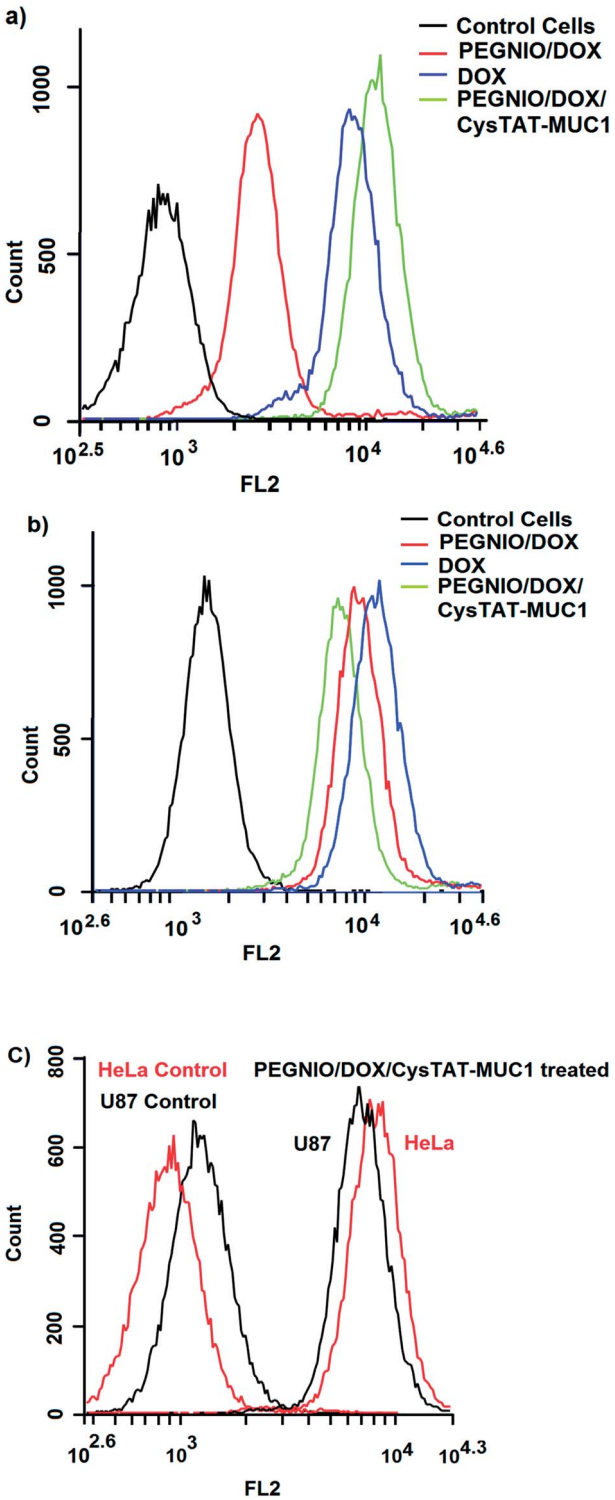

Fig. 3 Flow cytometric measurement of DOX uptake by HeLa (a) and U87 cells (b) after incubating with PEGNIO/DOX, PEGNIO/DOX/CysTAT–MUC1 and free DOX. Histogram of binding of PEGNIO/DOX/CysTAT–MUC1 to MUC1 positive HeLa cells and MUC1 negative U87 cells (c).

Cellular uptake and internalization

Flow cytometry was used to investigate the total DOX uptake by HeLa and U87 cells for different DOX formulations and to evaluate receptor mediated cell targeting. The cells were treated with samples for 2 h. Untreated control cells and treated cells were analyzed using a BD Accuri C6 flow cytometer. As shown in

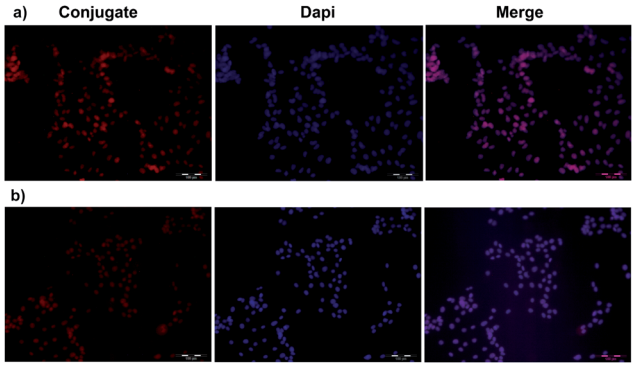

Fig. 4 Fluorescence microscopy images of HeLa (a) and U87 cells (b). PEGNIO/DOX/CysTAT–MUC1 was incubated with the cells for 4 h at 37 °C.

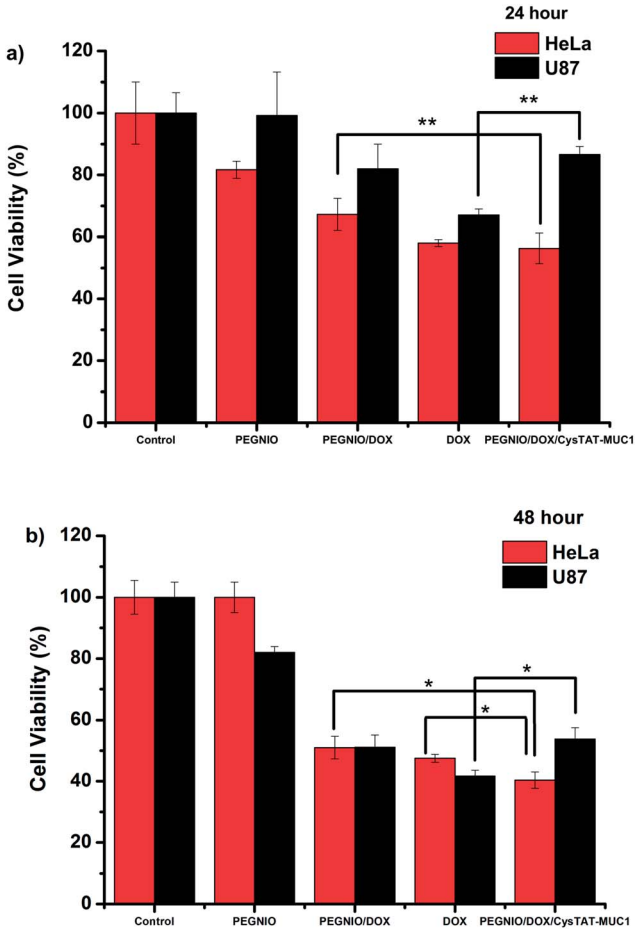

Fig. 5 Cytotoxicity of the free drug and niosomal formulations on HeLa and U87 cells. Cells were incubated with PEG/NIO, PEGNIO/DOX, PEGNIO/DOX/CysTAT–MUC1 and free DOX (equivalent concentration of loaded DOX) for 24 h (a) and for 48 h (b). MTT assay was applied. Error bars represent the standard deviation from the mean ($N = 3$). Data were analyzed using paired t-test, and $^{*}p < 0.05$, $^{**}p < 0.01$ was considered significant and very significant respectively.

Fig. 3a, the cellular DOX level for PEGNIO/DOX/CysTAT–MUC1 in HeLa cells was higher than that of PEGNIO/DOX and free DOX. Free DOX enters the cells by diffusion, leading to higher drug levels than found with the PEGNIO/DOX. After encapsulation of DOX in PEGNIO, the DOX uptake by diffusion is reduced.[49] In the case of U87 cells, the uptake of free DOX was higher than PEGNIO/DOX/CysTAT–MUC1 (Fig. 3b). Fig. 3c indicates that the synthesized PEGNIO/DOX/CysTAT–MUC1 conjugate bound to MUC1 positive HeLa cell specifically. Nonspecific binding to U87 cells was also observed, but the fluorescence signals were lower than for HeLa cells. Cellular internalization of PEGNIO/DOX/CysTAT–MUC1 obtained by fluorescence microscopy analysis. DOX is a fluorescent drug and, it localizes to the nucleus in tumor cells.[50] Both cell lines were treated with PEGNIO/DOX/CysTAT–MUC1 for 4 h. The synthesized conjugate bound to HeLa cells, resulting in high fluorescence of the cell nucleus, thereby demonstrating successful internalization. In contrast, fluorescence was significantly lower for U87 cells, indicating some nonspecific uptake in U87 cells (Fig. 4a and b). Fluorescence microscopy images show results similar to flow cytometry analysis.

Cytotoxicity

The cytotoxicity of bare niosomes, drug loaded formulations and free DOX was investigated by MTT assay using HeLa and U87 cells. PEGNIO was practically nontoxic to HeLa and U87 cells with relative cell viabilities above 80% for both 24 and 48 h (Fig. 5). PEGNIO/DOX was less toxic than free DOX on both cell lines after 24 and 48 h. This can be explained by the reduced diffusive uptake of PEGNIO/DOX in comparison to free DOX (Fig. 3a and b).[49,51] Due to the conjugation of the targeting ligand to PEGNIO/DOX, PEGNIO/DOX/CysTAT–MUC1 was more toxic to HeLa cells than to U87 cells after 24 and for 48 h. Both, after 24 and 48 hours PEGNIO/DOX/CysTAT–MUC1 had less cytotoxic effect of on U87 cells in comparison with free DOX ($p < 0.01$ and $p < 0.05$ respectively). PEGNIO/DOX/CysTAT–MUC1 increased the cytotoxicty for HeLa cells in comparison to PEGNIO/DOX for 24 and 48 hours ($p < 0.01$ and $p < 0.05$ respectively). Moreover in comparison to free DOX, PEGNIO/DOX/CysTAT–MUC1 showed a significantly increased toxic effect on HeLa cells after 48 h. According to obtained results, it is clear that the aptamer conjugated niosomal formulation acted as a targeted DOX delivery platform for MUC1 expressing tumor cells.

Conclusions

The objective of this study was to develop an efficient aptamer targeted niosomal drug delivery system. For this aim, PEGNIO was successfully synthesized by the thin film hydration method. The model drug DOX was encapsulated into the vesicles, and the surface of the vesicles was decorated with cell penetrating peptides and MUC1 aptamer as a targeting ligand. The drug-loaded niosomes exhibit great potential as targeting drug carriers. The targeted drug-loaded nanoparticles show stronger cytotoxicity of the MUC1 receptor overexpressed HeLa cells. As

a conclusion, the formulation PEGNIO/DOX/CysTAT–MUC1 might be a promising and efficient strategy for the delivery of DOX to MUC1 overexpressed tumor cells.

Acknowledgements

Konrad Adenauer Foundation is acknowledged for the financial support to Didem Ag Seleci. Martina Weiß and Rebecca Joncyzk (Leibniz University of Hannover, Institute for Technical Chemistry) are also acknowledged for technical help during HPLC and PCR analysis.

Notes and references

1 L. Brannon-Peppas and J. O. Blanchette, *Adv. Drug Delivery Rev.*, 2004, **64**, 1649–1659.
2 A. Sankhyan and P. Pawar, *J. Appl. Pharm. Sci.*, 2012, **02**, 20–32.
3 D. Ag Seleci, M. Seleci, J.-G. Walter, F. Stahl and T. Scheper, *J. Nanomater.*, 2016, 13.
4 F. B. Barlas, B. Demir, E. Guler, A. M. Senisik, H. A. Arican, P. Unak and S. Timur, *RSC Adv.*, 2016, **6**, 30217–30225.
5 M. Hong, S. Zhu, Y. Jiang, G. Tang and Y. Pei, *J. Controlled Release*, 2009, **133**, 96–102.
6 R. Muzzalupo, L. Tavano and C. La Mesa, *Int. J. Pharm.*, 2013, **458**, 224–229.
7 L. Tavano, R. Muzzalupo, L. Mauro, M. Pellegrino, S. Ando and N. Picci, *Langmuir*, 2013, **29**, 12638–12646.
8 J. Park, P. M. Fong, J. Lu, K. S. Russell, C. J. Booth, W. M. Saltzman and T. M. Fahmy, *Nanomedicine*, 2009, **5**, 410–418.
9 A. I. Minchinton and I. F. Tannock, *Nat. Rev. Cancer*, 2006, **6**, 583–592.
10 E. Koren and V. P. Torchilin, *Trends Mol. Med.*, 2012, **18**, 385–393.
11 W. L. L. Munyendo, H. Lv, H. Benza-Ingoula, L. D. Baraza and J. Zhou, *Biomolecules*, 2012, **2**, 187–202.
12 M. Lindgren, K. Rosenthal-Aizman, K. Saar, E. Eiriksdottir, Y. Jiang, M. Sassian, P. Östlund, M. Hällbrink and Ü. Langel, *Biochem. Pharmacol.*, 2006, **71**, 416–425.
13 M. Seleci, D. A. Seleci, M. Ciftci, D. Odaci Demirkol, F. Stahl, S. Timur, T. Scheper and Y. Yagci, *Langmuir*, 2015, **31**, 4542–4551.
14 S. Deshayes, M. C. Morris, G. Divita and F. Heitz, *Cell. Mol. Life Sci.*, 2005, **62**, 1839–1849.
15 M. Mano, C. Teodosio, S. Simoes, d. L. M. Pedroso and A. Paiva, *Biochem. J.*, 2005, **390**, 603–612.
16 N. Schmidt, A. Mishra, G. H. Lai and G. C. L. Wong, *FEBS Lett.*, 2010, **584**, 1806–1813.
17 B. R. Liu, Y.-W. Huang, H.-J. Chiang and H.-J. Lee, *J. Nanosci. Nanotechnol.*, 2010, **10**, 7897–7905.
18 E. Vives, J. Schmidt and A. Pelegrin, *Biochim. Biophys. Acta, Rev. Cancer*, 2008, **1786**, 126–138.
19 J. Taylor-Papadimitriou, J. Burchell, D. W. Miles and M. Dalziel, *Biochim. Biophys. Acta, Mol. Basis Dis.*, 1999, **1455**, 301–313.
20 Z. Cao, R. Tong, A. Mishra, W. Xu, G. C. L. Wong, J. Cheng and Y. Lu, *Angew. Chem., Int. Ed.*, 2009, **48**, 6494–6498.
21 T. Chen, M. I. Shukoor, Y. Chen, Q. Yuan, Z. Zhu, Z. Zhao, B. Gulbakan and W. Tan, *Nanoscale*, 2011, **3**, 546–556.
22 Z. Liu, H. Zhao, L. He, Y. Yao, Y. Zhou, J. Wu, J. Liu and J. Ding, *RSC Adv.*, 2015, **5**, 16931–16939.
23 A. Ozer, J. M. Pagano and J. T. Lis, *Mol. Ther.–Nucleic Acids*, 2014, **3**, e183.
24 C. S. M. Ferreira, C. S. Matthews and S. Missailidis, *Tumor Biol.*, 2006, **27**, 289–301.
25 Y. Hu, J. Duan, Q. Zhan, F. Wang, X. Lu and X.-D. Yang, *PLoS One*, 2012, **7**, e31970.
26 C. Yu, Y. Hu, J. Duan, W. Yuan, C. Wang, H. Xu and X.-D. Yang, *PLoS One*, 2011, **6**, e24077.
27 L. Tan, K. G. Neoh, E. T. Kang, W. S. Choe and X. Su, *Macromol. Biosci.*, 2011, **11**, 1331–1335.
28 M. N. Azmin, A. T. Florence, R. M. Handjani-Vila, J. F. B. Stuart, G. Vanlerberghe and J. S. Whittaker, *J. Pharm. Pharmacol.*, 1985, **37**, 237–242.
29 Z.-X. Liao, E.-Y. Chuang, C.-C. Lin, Y.-C. Ho, K.-J. Lin, P.-Y. Cheng, K.-J. Chen, H.-J. Wei and H.-W. Sung, *J. Controlled Release*, 2015, **208**, 42–51.
30 J. Takasaki and S. M. Ansell, *Bioconjugate Chem.*, 2006, **17**, 438–450.
31 L. Tavano, R. Aiello, G. Ioele, N. Picci and R. Muzzalupo, *Colloids Surf., B*, 2014, **118**, 7–13.
32 S. B. Shirsand, M. S. Para, D. Nagendrakumar, K. M. Kanani and D. Keerthy, *Int. J. Pharm. Invest.*, 2012, **2**, 201–207.
33 G. Wei, S. Xiao, D. Si and C. Liu, *Biomed. Chromatogr.*, 2008, **22**, 1252–1258.
34 A. Shrivastava and V. B. Gupta, *Chron. Young Sci.*, 2011, **2**, 21–25.
35 R. Bongartz, D. Ag, M. Seleci, J.-G. Walter, E. E. Yalcinkaya, D. O. Demirkol, F. Stahl, S. Timur and T. Scheper, *J. Mater. Chem. B*, 2013, **1**, 522–528.
36 G. Minotti, P. Menna, E. Salvatorelli, G. Cairo and L. Gianni, *Pharmacol. Rev.*, 2004, **56**, 185–229.
37 P. Mohan and N. Rapoport, *Mol. Pharmaceutics*, 2010, **7**, 1959–1973.
38 B. Haley and E. Frenkel, *Urologic Oncology: Seminars and Original Investigations*, 2008.
39 T. M. Allen and P. R. Cullis, *Science*, 2004, **303**, 1818–1822.
40 G. T. Hermanson, *Bioconjugate Techniques*, Academic press, 2nd edn, 2008.
41 Y. Li, M. Kröger and W. K. Liu, *Biomaterials*, 2014, **35**, 8467–8478.
42 J. V. Jokerst, T. Lobovkina, R. N. Zare and S. S. Gambhir, *Nanomedicine*, 2011, **6**, 715–728.
43 N. O. Sahin, in *Nanomaterials and Nanosystems for Biomedical Applications*, Springer, 2007, pp. 67–81.
44 M. Bragagni, N. Mennini, C. Ghelardini and P. Mura, *J. Pharm. Pharm. Sci.*, 2012, **15**, 184–196.
45 G. A. Hughes, *Nanomedicine*, 2005, **1**, 22–30.
46 J. Qi, P. Yao, F. He, C. Yu and C. Huang, *Int. J. Pharm.*, 2010, **393**, 177–185.
47 C. t. S. M. Ferreira, M. C. Cheung, S. Missailidis, S. Bisland and J. Gariepy, *Nucleic Acids Res.*, 2009, **37**, 866–876.

48 M. S. Syrkina, M. A. Rubtsov, D. M. Potashnikova, Y. D. Kondratenko, A. A. Dokrunova and V. P. Veiko, *Acta Naturae*, 2014, **6**, 62–70.
49 X.-B. Xiong, Y. Huang, W.-l. Lu, X. Zhang, H. Zhang, T. Nagai and Q. Zhang, *J. Controlled Release*, 2005, **107**, 262–275.
50 A. D. Heibein, B. Guo, J. A. Sprowl, D. A. MacLean and A. M. Parissenti, *BMC Cancer*, 2012, **12**, 381.
51 X. Li, L. Ding, Y. Xu, Y. Wang and Q. Ping, *Int. J. Pharm.*, 2009, **373**, 116–123.